Influence of the image charge effect on excitonic energy structure in organic-inorganic multiple quantum well crystals

Hidetsugu Takagi, Hideyuki Kunugita, and Kazuhiro Ema
Department of Physics, Sophia University, 7-1 Kioicho, Chiyoda-ku, Tokyo 102-8554, Japan
(Received 30 August 2012; revised manuscript received 9 February 2013; published 19 March 2013)

We have experimentally compared the excitonic properties of hybrid multiple quantum wells, $(C_6H_5\text{-}C_2H_4NH_3)_2PbBr_4$ and $(C_4H_9NH_3)_2PbBr_4$, using photoluminescence, reflection, and photoluminescence excitation measurements. We focused on the contribution of the image charge effect (ICE) to the excitonic energy structure in these materials which have different dielectric constants of the barrier layers. We have found that the binding energies of the 2*s* and 3*s* excitons are considerably enhanced by ICE, while the contribution of ICE to the 1*s* excitons is smaller because of the small Bohr radius, which is comparable to the well width.

DOI: 10.1103/PhysRevB.87.125421 PACS number(s): 78.67.De, 71.35.−y, 71.36.+c

I. INTRODUCTION

Organic-inorganic hybrid semiconductors have attracted much attention from the viewpoint of basic science as well as for applications in optoelectronics.[1] A suitable combination of organic and inorganic materials can overcome some of the limitations present when they are used separately. For example, the resonant coupling of excitons between organic molecules and inorganic semiconductor quantum wells (QWs) can lead to simultaneous high oscillator strength and strong optical nonlinearity.[2,3] For such applications[4–6] we need to clarify the fundamental properties of the excitons in QWs, focusing on the characteristic property of the hybrid materials.

The layered perovskite-type organic-inorganic QW materials form self-organized two-dimensional (2D) systems, where inorganic semiconductor well layers are sandwiched by organic barrier layers.[7,8] These materials are being considered for several optoelectronic applications.[9–14] Moreover, since these materials have no well-width fluctuation and no lattice mismatch, they are suitable for the fundamental study of the excitonic properties in 2D systems. Due to the ideal 2D hybrid structure, excitons are tightly confined in the inorganic monomolecular layer of $[PbX_6]^{4-}$ (X = I,Br,Cl) octahedra placed between organic barrier layers consisting of alkyl-ammonium or phenylethyl-ammonium chains.[8] It is also known that the electronic coupling between the adjacent inorganic well layers is almost nonexistent because of a high potential barrier of the organic layers.[8] In these materials, it has been reported that the binding energies of the exciton and the biexciton are extremely large (E_{ex} = 350–480 meV, E_M = 40–60 meV),[15–17] which are the largest values ever reported. Thanks to the large exciton binding energies, the longitudinal-transverse (LT) splitting also becomes extremely large (70–100 meV). Such a huge binding energy is enhanced not only by the quantum confinement effect (QCE) but also by the image charge effect (ICE).[18,19] If we assume the 2D limit (well width is zero and barrier potential is infinity) of a single QW, the exciton binding energy relative to the three-dimensional (3D) case will be enhanced as[19]

$$E_{ex}^{2D} = 4\left(\frac{\varepsilon_w}{\varepsilon_b}\right)^2 E_{ex}^{3D}, \quad (1)$$

where ε_w and ε_b are the dielectric constants of the well layer and the barrier layer, respectively. E_{ex}^{3D} is the binding energy of the corresponding 3D excitons. In the 2D limit, the enhancement factor of 4 is that of perfect QCE and the squared ratio of the dielectric constants results from the perfect ICE for a single QW.

For organic-inorganic QW materials, the ICE becomes dominant, since the dielectric constant of the barrier layers (ε_b = 2–3.5) is much smaller than that of the well layers (ε_w = 4.8).[16,20,21] This is in strong contrast to inorganic semiconductors, in which the differences of the dielectric constants are usually less than 10%. Therefore, ICE is one of the characteristic properties of the hybrid materials. Since the physical mechanism of ICE is a reduction in Coulomb screening due to the small dielectric constant of the barrier layer, the magnitude of the effect depends on the amount of leakage of the electric lines of the Coulomb force. In other words, it depends on the relationship between the exciton Bohr radius and the well width. Therefore, the influences of ICE on n = 1 excitons and n = 2 excitons are expected to be different. Although there are several studies of ICE in the organic-inorganic hybrid materials,[17,20,22,23] studies exploring the different effect of ICE on 1*s*, 2*s*, and 3*s* excitons are very limited in number.[17] In this study, we have investigated the difference in the contribution of ICE, not only due to the different barrier materials, but also among the 1*s*, 2*s*, and 3*s* excitons.

II. EXPERIMENT

Among the layered perovskite-type organic-inorganic QW materials, we focus on $(C_6H_5\text{-}C_2H_4NH_3)_2PbBr_4$ (hereafter denoted as "PhEPbBr4") and $(C_4H_9NH_3)_2PbBr_4$ (hereafter denoted as "C4PbBr4"). These materials have the same well layers with the same thickness (l_w = 0.5 nm) (Ref. 16) and the same dielectric constant (ε_w = 4.8) but the barrier layers have different dielectric constants (PhEPbBr4: ε_b = 3.32; C4PbBr4: ε_b = 2.1–2.4).[7,20] In addition, we have confirmed that both PhEPbBr4 and C4PbBr4 show no structural phase transition below room temperature. Therefore, these materials are suitable for the study of ICE in 2D systems at low temperature.

The samples used in this study were single crystals of PhEPbBr4 and C4PbBr4 prepared by a chemical synthetic method. Both samples have a size of about 2×2 mm^2 and were kept at 10 K for the measurements. We measured photoluminescence (PL), reflection, and photoluminescence excitation (PLE) spectra around the excitonic resonance. The excitation light source for the PL experiments was a second harmonic generation of a pulse from an optical parametric amplifier seeded by an amplified mode-locked Ti:Al_2O_3 laser at a repetition rate of 10 kHz. For PLE experiments, we used a Xe lamp filtered by a spectrometer as the excitation light. The signals were detected with an optical multichannel analyzer.

III. RESULTS AND DISCUSSION

Figure 1 shows the excitation intensity dependence of PL spectra for C4PbBr4 and PhEPbBr4 at 10 K with an excitation energy of 3.542 eV. In our previous study, four main peaks in the PL spectra of C4PbBr4 were already assigned to be Γ_5^-, Γ_2^-, Γ_1^-, and M peaks.[15,24] Γ_5^- is the emission from the singletlike excitons (bright excitons) and Γ_1^-, Γ_2^- are from the tripletlike excitons (dark excitons). The reason why the emissions from the dark excitons are stronger than those from the bright excitons is that the populations of the dark-exciton states are much larger than that of the bright-exciton state due to a fast spin relaxation from the bright-exciton state to the dark-exciton states. The energy splitting between Γ_5^- and Γ_1^- is caused by the exciton exchange interaction. These anomalously large exchange energies (>25 meV) are due to the small 2D-exciton Bohr radius, which is a consequence of both the strong QCE and ICE. M is the emission from the biexciton state to the Γ_5^- state. The energy differences between M and Γ_5^- for both samples show extremely large biexciton binding energies of $\sim$ 60 meV.

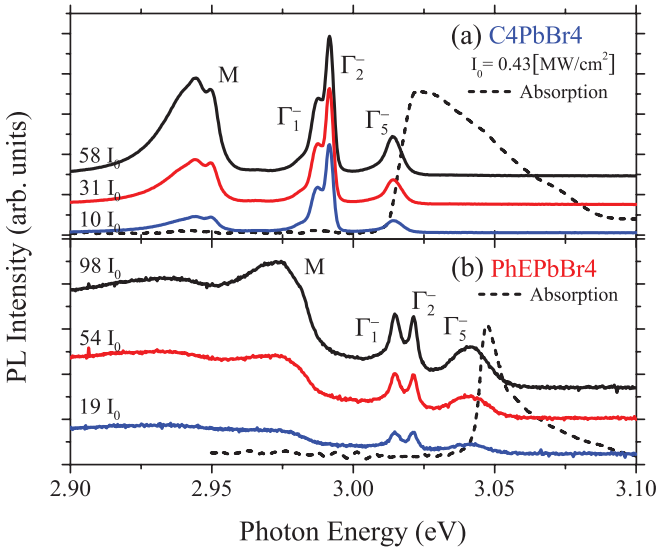

FIG. 1. (Color online) Photoluminescence spectra of (a) C4PbBr4 and (b) PhEPbBr4 single crystals at 10 K for various excitation intensities. There are four main peaks in both samples. The assignments of these four peaks are described in the text. Dashed lines show absorption spectra obtained by the Kramers-Kronig relation of reflection spectra.

We can see from Fig. 1 that the PL spectrum of PhEPbBr4 is very similar to that of C4PbBr4, although there is a broad peak on the lower side of the M peak probably due to impurity states. Therefore, we can assign the four peaks in Fig. 1(b) to be the same as those in Fig. 1(a). All excitonic emission lines of PhEPbBr4 are found to be located at higher energies than those of C4PbBr4. For example, the Γ_5^- peak of C4PbBr4 is located at 3.02 eV, while that of PhEPbBr4 is located at 3.04 eV.

In these materials, it is difficult to estimate the band-gap energy from the optical data, because the oscillator strength of the excitons is so strong that the band-edge absorption becomes invisible. Tanaka estimated the exciton binding energy of C4PbBr4 to be 480 meV assuming that the band-gap energy is 3.5 eV. Since this assumption was not based on clear optical data, but only from the suppression of the electroabsorption signals above 3.5 eV, it seems poorly founded. However, Tanaka showed that the ns-exciton ($n \geqslant 2$) energies in the similar materials C6PbI4 obey the ideal 2D Wannier series.[17] Therefore, we can estimate the band-gap energy if we obtain the energy positions of the 2s and 3s excitons. To obtain the 2s and 3s exciton energies, we performed PLE and reflection experiments.

Figure 2 shows PLE and reflection spectra for both samples at 10 K. For the PLE spectra we monitored the Γ_2^- emission. The stop bands due to the LT splitting are clearly observed in the reflection spectra. Although C4PbBr4 and PhEPbBr4 are not bulk samples but multi-QW (MQW) samples, it is known that, if the number of QWs is sufficiently large, the MQW polaritons have the same feature as that of the bulk exciton polaritons.[25] Around the 1s exciton resonance, the PLE signals decrease in the stop band region (denoted as

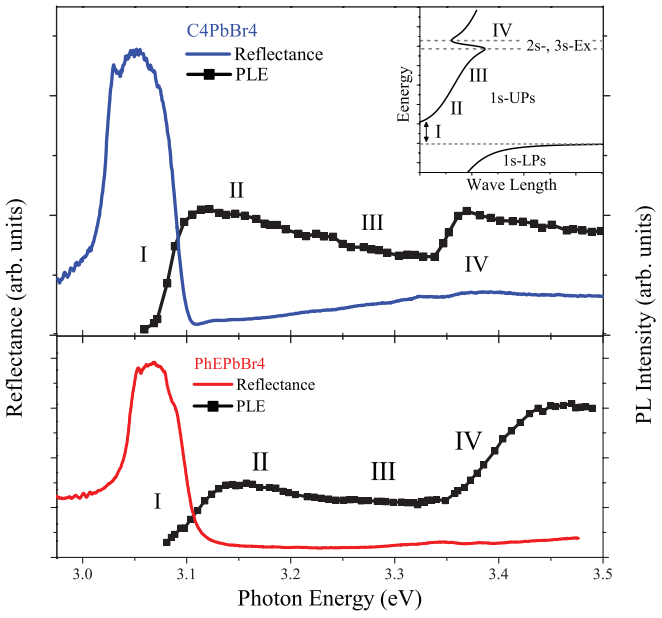

FIG. 2. (Color online) (Color line) Reflection and PLE spectra of (a) C4PbBr4 and (b) PhEPbBr4 single crystals at 10 K. The features in the PLE (denoted I–IV) are explained in the text. The inset shows a schematic of the polariton dispersion, in which the 2s and 3s exciton resonances are merged considering the resolution in the PLE experiments.

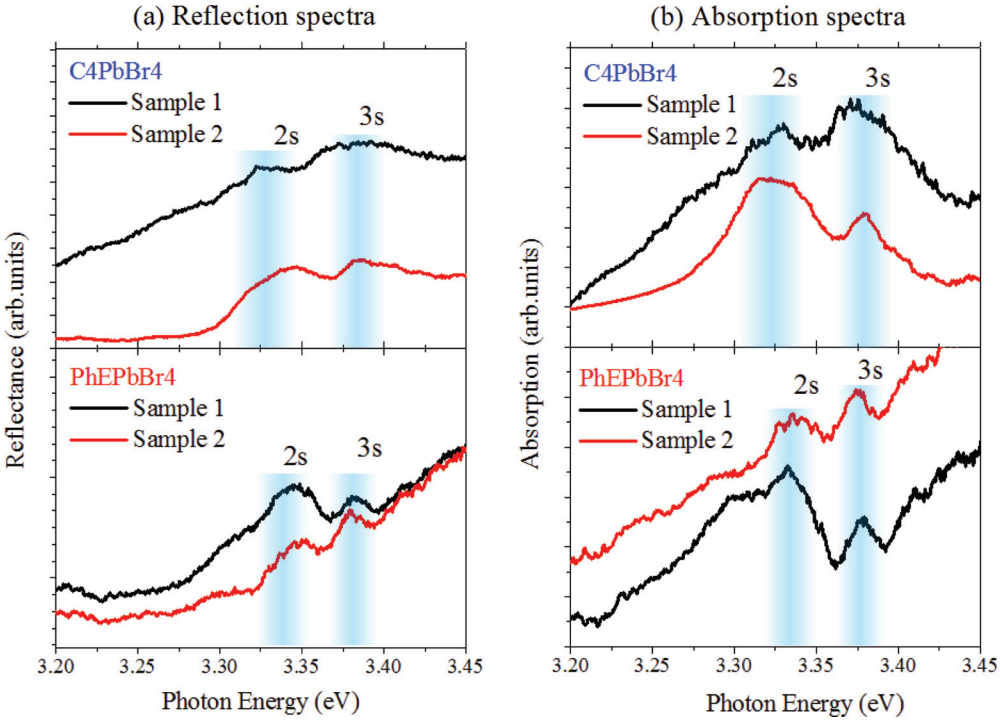

FIG. 3. (Color online) (a) Expanded views of the reflection spectra around 2*s* and 3*s* exciton resonances. (b) Absorption spectra obtained by the Kramers-Kronig analysis of the reflection spectra. Sample 1 is the same sample shown in Fig. 1.

I in Fig. 2) and increase toward the longitudinal energy of the exciton (denoted as II in Fig. 2). Above the 1*s* exciton resonance, the signals from the upper-branch polaritons (UPs) appear due to LO phonon scatterings from the UPs to the lower-branch polaritons (LPs). The signals from UPs decrease with an increase in the excitation energy (denoted as III in Fig. 2) because of a decrease in the excitonlike component of the UPs. However, as we can see from Fig. 2, the decreases of the PLE signals are slow and the intensities remain at some level over a wide energy range. This indicates that the UPs contain considerable excitonlike components over such a wide energy range. Since, in general, polaritons contain considerable excitonlike components over an energy range that can be more than ten times their LT-splitting energies, the range becomes several hundreds of meV for these materials.[26]

We can see that the PLE signals increase abruptly around 3.33 eV (denoted as IV in Fig. 2). This is because the excitonlike components of the UPs increase again due to the 2*s* and 3*s* exciton resonances. Although each respective peak of the 2*s* and 3*s* exciton resonances could not be identified because of the resolution limit in our PLE experiments (20–30 meV), it is clear that the excitonlike components exist in this region. In addition, we can find some structures around 3.33–3.34 eV in the reflection spectra for both C4PbBr4 and PhEPbBr4. Figure 3(a) shows an expanded view of the reflection spectra, focusing on these structures. We can see that there are two small peaks which are reasonably assigned to the 2*s* and 3*s* resonances. To confirm that these peaks are not caused by experimental noise, Fig. 3(a) also shows the data from another sample. We found that all data from other samples have two peaks in this region.

By using the Kramers-Kronig relation, we obtained the absorption spectra from the reflection spectra. The obtained absorption spectra around the 1*s* exciton resonance are plotted together with the PL spectra in Fig. 1 and those around the 2*s* and 3*s* exciton resonances are shown in Fig. 3(b). Since the absorption spectra around the 2*s* and 3*s* exciton resonances are somewhat noisy, we used a peak-analysis method for several sets of data including ones other than those shown in the figures. The peak analyzer showed that there were two main peaks corresponding to the absorption peaks of the 2*s* and 3*s* excitons. From the obtained absorption peaks we can estimate the energy positions of the exciton resonances to be 3.022 (±0.001) eV (1*s*), 3.316 (±0.005) eV (2*s*), and 3.379 (±0.004) eV (3*s*) for C4PbBr4; and 3.047 (±0.001) eV (1*s*), 3.333 (±0.002) eV (2*s*), and 3.378 (±0.003) eV (3*s*) for PhEPbBr4.

In Fig. 4, the estimated resonance energies of the ns excitons are plotted as a function of $1/(n-1/2)^2$. Since the 2*s* and 3*s* exciton energies can be described by a simple 2D Wannier series, we can draw lines passing through the 2*s* and 3*s* energies described by

$$E_n = E_g - \mathrm{Ry}^{(\mathrm{ICE})}/(n-1/2)^2, \qquad (2)$$

where $\mathrm{Ry}^{(\mathrm{ICE})}$ indicates the excitonic Rydberg energy, including the ICE effect. From these lines we can estimate the band-gap energy E_g, $\mathrm{Ry}^{(\mathrm{ICE})}$, and then the binding energies of the excitons. The estimated values are summarized in Table I.[27] By comparing $\mathrm{Ry}^{(\mathrm{ICE})}$ with the excitonic Rydberg energy of the three-dimensional analog material of the well structure, $CH_3NH_3PbBr_4$ ($\mathrm{Ry}^{(3D)} = 76$ meV),[21] we can discuss the enhancement factor of ICE. We can see that the estimated values of $\mathrm{Ry}^{(\mathrm{ICE})}$ are much larger than that of $\mathrm{Ry}^{(3D)}$, which clearly indicates that ICE is fairly effective in these

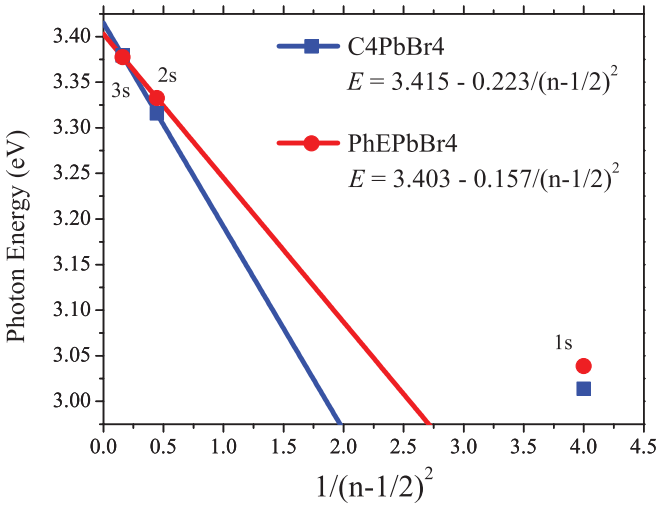

FIG. 4. (Color online) Observed resonance energies of Wannier-series excitons in C4PbBr4 and PhEPbBr4 as a function of $1/(n-1/2)^2$. The solid line shows the fitting based on a simple two-dimensional Wannier exciton model.

materials. The enhancement factor $F^{(\mathrm{ICE})}$, which we define by $\mathrm{Ry}^{(\mathrm{ICE})}/\mathrm{Ry}^{(3\mathrm{D})}$, can be estimated to be $F^{(\mathrm{ICE})} = 0.223/0.076 = 2.93$ for C4PbBr4 and $F^{(\mathrm{ICE})} = 2.08$ for PhEPbBr4. The larger value of $F^{(\mathrm{ICE})}$ for C4PbBr4 is considered to originate from the smaller value of the dielectric constant of the barrier layer. Although this seems like a clear demonstration of the differences in the contributions of ICE in these two materials, it is prudent to carefully consider this result, as discussed below.

The obtained values of $F^{(\mathrm{ICE})}$ are smaller than those expected from the squared ratio of the dielectric constant $(4.8/2.1)^2 = 5.2$ and $(4.8/3.32)^2 = 2.1$, which indicates that the contribution of ICE is not following the perfect 2D limit for a single QW described by Eq. (1). This is quite reasonable because these materials are not single-QW materials but MQW materials. In the case of MQW materials, the ratio of the barrier width and the well width influences the magnitude of ICE, therefore we should use the effective dielectric constant averaged over the MQW,

$$\varepsilon^* = \sqrt{\varepsilon_{\mathrm{w}}\varepsilon_{\mathrm{b}}\frac{(\varepsilon_{\mathrm{w}}l_{\mathrm{w}} + \varepsilon_{\mathrm{b}}l_{\mathrm{b}})}{(\varepsilon_{\mathrm{b}}l_{\mathrm{w}} + \varepsilon_{\mathrm{w}}l_{\mathrm{b}})}}, \tag{3}$$

where l_{b} and l_{w} are the barrier and well widths, respectively. By substituting the actual values, i.e., $l_{\mathrm{b}} = 0.8$ nm for C4PbBr4 and $l_{\mathrm{b}} = 1.0$ nm for PhEPbBr4,[20,28] we obtain $\varepsilon^* = 2.9$ and 3.8, respectively. If we use the effective dielectric constants, the expected enhancement factors become $(4.8/2.9)^2 = 2.6$ for C4PbBr4 and $(4.8/3.8)^2 = 1.6$ for PhEPbBr4. It should be noted that ε^* is appropriate if the material is assumed to be uniform continuous matter, therefore an estimation for the enhancement of ICE using ε^* leads to an underestimation. On the other hand, the estimation using Eq. (1) is appropriate if all electric lines of the Coulomb force are assumed to lie in the barrier, therefore this leads to an overestimation of the enhancement of ICE. Since the dielectric constant might not be a well-defined parameter for an extremely narrow QW, as in the present case, we can only suggest that the enhancement factor of ICE should range between the underestimated and overestimated values. According to this criterion, the enhancement factors should lie in the range from 2.6 to 5.2 for C4PbBr4 and from 1.6 to 2.1 for PhEPbBr4. We have found that the observed values of $F^{(\mathrm{ICE})}$ lie in these ranges for both materials. This is a clear demonstration of the differences in the contribution of ICE due to the different barrier materials. The observed value of $F^{(\mathrm{ICE})}$ for C4PbBr4 is close to the underestimated value (continuous approximation case), while the one for PhEPbBr4 is close to the overestimated value (perfect-single-QW approximation case). However, we prefer to avoid a detailed discussion of this point, because the dielectric constants used here are not completely precise, having been estimated from optical interference fringes by a simple calculation model. The important point here is that the observed $F^{(\mathrm{ICE})}$ for both materials lie in the range between the underestimated and overestimated values.

TABLE I. Comparison of the excitonic parameters in PhEPbBr4 and C4PbBr4.

	E_{g}	$\mathrm{Ry}^{(\mathrm{ICE})}$ (eV)	$F^{(\mathrm{ICE})}$ (meV)	$E_{\mathrm{b}}^{(1s)}$ (meV)
C4PbBr4	~3.42	240	5.2	393
PhEPbBr4	~3.40	170	2.1	356

From Fig. 4, we can readily see that the 1s exciton resonance energies for both C4PbBr4 and PhEPbBr4 deviate from Eq. (2) to the higher-energy side. This feature was already reported in Ref. 22, and means that the contribution of ICE to the 1s excitons is much smaller than that to the 2s and 3s excitons. This is reasonable because the well width is finite and comparable to the Bohr radius of the 1s excitons. Although both QCE and ICE work well for the exciton confinement in these materials, the contribution of ICE becomes saturated if the Bohr radius becomes small enough to become comparable to the well width. Therefore, the excitonic energy structure with ICE does not obey the hydrogenic energy series of the Wannier excitons. This means that we can control the excitonic energy structure by choosing the dielectric constant of the barrier layer or by changing the well width. This unique feature brings us another way to tune the resonant coupling between the inorganic and organic parts in the hybrid materials.

IV. SUMMARY

In summary, we have clearly demonstrated that ICE is dominant in both C4PbBr4 and PhEPbBr4, and the amount of the effect varies with the dielectric constant of the barrier layer. We have shown that the binding energies of the 2s exciton are considerably enhanced by ICE, while the contribution of ICE to the 1s excitons is smaller than that to the 2s excitons because of the small Bohr radius comparable to the well width. This feature can be used for tuning the excitonic energy structure to couple the resonance between organic and inorganic materials.

ACKNOWLEDGMENTS

This work was supported by Grants-in-Aid for Scientific Research, Grants No. 23104725 and No. 23654106, from the Ministry of Education, Culture, Sports, Science and Technology, Japan.

[1]See, for example, V. M. Agranovich, Y. N. Gartstein, and M. Litinskaya, Chem. Rev. **111**, 5179 (2011), and references therein.
[2]V. Agranovich, R. Atanasov, and F. Bassani, Solid State Commun. **92**, 295 (1994).
[3]O. Roslyak and J. L. Birman, Phys. Rev. B **75**, 245309 (2007).
[4]S. Blumstengel, S. Sadofev, C. Xu, J. Puls, and F. Henneberger, Phys. Rev. Lett. **97**, 237401 (2006).
[5]G. Itskos, G. Heliotis, P. G. Lagoudakis, J. Lupton, N. P. Barradas, E. Alves, S. Pereira, I. M. Watson, M. D. Dawson, J. Feldmann, R. Murray, and D. D. C. Bradley, Phys. Rev. B **76**, 035344 (2007).
[6]K. Ema, M. Inomata, Y. Kato, H. Kunugita, and M. Era, Phys. Rev. Lett. **100**, 257401 (2008).
[7]T. Ishihara, in *Optical Properties of Low-dimensional Materials*, edited by T. Ogawa and Y. Kanemitsu (World Scientific, Singapore, 1995), Chap. 6.
[8]T. Ishihara, J. Takahashi, and T. Goto, Phys. Rev. B **42**, 11099 (1990).
[9]G. Lanty, J. S. Lauret, E. Deleporte, S. Bouchoule, and X. Lafosse, Appl. Phys. Lett. **93**, 081101 (2008).
[10]T. Fujita, Y. Sato, T. Kuitani, and T. Ishihara, Phys. Rev. B **57**, 12428 (1998).
[11]J. Ishi, H. Kunugita, K. Ema, T. Ban, and T. Kondo, Appl. Phys. Lett. **77**, 3487 (2002).
[12]M. Era, S. Morimoto, and S. Saito, Appl. Phys. Lett. **65**, 676 (1994).
[13]K. Shibuya, M. Koshimizu, H. Murakami, Y. Muroya, Y. Katsumura, and K. Asai, Jpn. J. Appl. Phys. **43**, L1333 (2004).
[14]M. Shimizu and T. Ishihara, Appl. Phys. Lett. **80**, 2836 (2002).
[15]Y. Kato, D. Ichii, K. Ohashi, H. Kunugita, K. Ema, K. Tanaka, T. Takahashi, and T. Kondo, Solid State Commun. **128**, 15 (2003).
[16]K. Tanaka, T. Takahashi, T. Kondo, K. Umeda, K. Ema, T. Umebayashi, K. Asai, K. Uchida, and N. Miura. Jpn. J. Appl. Phys. **44**, 5923 (2005).
[17]K. Tanaka, T. Takahashi, T. Kondo, T. Umebayashi, K. Asai, and K. Ema, Phys. Rev. B **71**, 045312 (2005).
[18]E. Hanamura, N. Nagaosa, M. Kumagai, and T. Takagahara, Mater. Sci. Eng. B **1**, 255 (1988).
[19]L. V. Keldysh, Pis'ma Zh. Eksp. Teor. Fiz. **29**, 716 (1979) [JETP Lett. **29**, 658 (1979)].
[20]X. Hong, T. Ishihara, and A. V. Nurmikko, Phys. Rev. B **45**, 6961 (1992).
[21]K. Tanaka, T. Takahashi, T. Ban, T. Kondo, K. Uchida, and N. Miura, Solid State Commun. **127**, 619 (2003).
[22]E. A. Muljarov, S. G. Tikhodeev, N. A. Gippius, and T. Ishihara, Phys. Rev. B **51**, 14370 (1995).
[23]M. Shimizu, J.-I. Fujisawa, and J. Ishi-Hayase, Phys. Rev. B **71**, 205306 (2005).
[24]K. Ema, K. Umeda, M. Toda, C. Yajima, Y. Arai, H. Kunugita, D. Wolverson, and J. J. Davies, Phys. Rev. B **73**, 241310(R) (2006).
[25]R. Tamaki, Y. Arai, D. Ichikawa, M. Inoue, H. Kunugita, and K. Ema, J. Lumin. **128**, 842 (2008).
[26]C. F. Klingshirn, *Semiconductor Optics*, 3rd ed. (Springer-Verlag, Berlin, 2007), p. 302.
[27]Although the exciton binding energy should be probably determined by the energy difference between the band gap and the triplet exciton energy, it is commonly taken as the difference between the band gap and the bright exciton.
[28]Y. Tabuchi, K. Asai, M. Rikukawa, K. Sanui, and K. Ishigure, J. Phys. Chem. Solids **61**, 837 (2000).